



Pyrrolidine-pyrazole ureas as potent and selective inhibitors of 11 β -hydroxysteroid-dehydrogenase type 1

Olivier Venier^{a,*}, Cécile Pascal^a, Alain Braun^a, Claudie Namane^a, Patrick Mougenot^a, Olivier Crespin^a, François Pacquet^a, Cécile Mougenot^a, Catherine Monseau^a, Bénédicte Onofri^a, Rommel Dadjai-Faihun^a, Céline Leger^a, Majdi Ben-Hassine^a, Thao Van-Pham^a, Jean-Luc Ragot^a, Christophe Philippo^a, Stefan Güssregen^b, Christian Engel^b, Géraldine Farjot^a, Lionel Noah^a, Karima Maniani^a, Eric Nicolai^{a,*}

^aSanofi-aventis R&D, 1 Avenue Pierre Brossollette, 91385 Chilly-Mazarin, France

^bSanofi-aventis Deutschland GmbH, Industriepark Hoechst, 65926 Frankfurt am Main, Germany

ARTICLE INFO

Article history:

Received 18 January 2011

Revised 25 February 2011

Accepted 27 February 2011

Available online 23 March 2011

Keywords:

11 β -Hydroxysteroid-dehydrogenase type 1

11 β -HSD-1 inhibitors

Metabolic syndrome

Urea

Pyrrolidine-pyrazole

Pharmacodynamic ex vivo assay

ABSTRACT

A High Throughput Screening campaign allowed the identification of a novel class of ureas as 11 β -HSD1 inhibitors. Rational chemical optimization provided potent and selective inhibitors of both human and murine 11 β -HSD1 with an appropriate ADME profile and ex vivo activity in target tissues.

© 2011 Elsevier Ltd. All rights reserved.

11 β -Hydroxy steroid dehydrogenase type 1 (11 β -HSD1) converts the biologically inactive glucocorticoids, cortisone (in man) and 11-dehydrocorticosterone (in rodents), into their biologically active metabolites, respectively cortisol and corticosterone, which are known to act as functional antagonists of insulin in several target organs and tissues such as the liver, muscle, and adipose tissue (Fig. 1).¹ There is evidence implicating an excess of cortisol in tissues as a primary driver of insulin resistance and a critical point for disease intervention.² Liver- or adipose tissue-specific overexpression of 11 β -HSD1 in transgenic mice produces a phenotype closely resembling human type 2 diabetes mellitus.³ Reduction of intracellular corticosterone levels in rodents as a result of pharmacological inhibition of 11 β -HSD1 reverses manifestations of altered metabolic parameters including ectopic fat storage, diabetes, dyslipidemia and atherosclerosis.⁴ Both 11 β -HSD1 expression and activity are up-regulated in the adipose tissue of obese, insulin-resistant or diabetic humans.⁵ Inhibition of 11 β -HSD1 therefore offers potential as a novel therapy to lower intracellular cortisol concentrations and thereby enhance insulin sensitivity and hepatic lipid catabolism in type 2 diabetes, obesity, and hyperlipidemia.

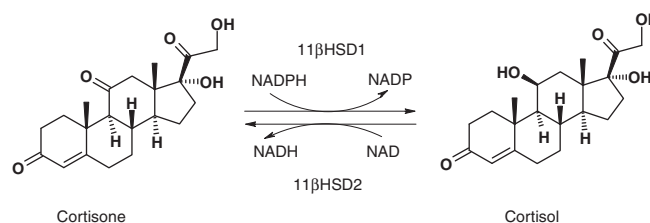


Figure 1. Interconversion of cortisone and cortisol by 11 β -HSD1 and 11 β -HSD2 enzymes.

Two isoforms of 11 β -HSD are known, the products of distinct genes: 11 β -HSD1 is primarily expressed in the liver and adipose tissue, the other isoform, 11 β -HSD2, is located mainly in the kidney.⁶ 11 β -HSD2 converts active glucocorticoids (such as cortisol and corticosterone) into inactive cortisone or 11-dehydrocorticosterone. Any potential drug aimed at inhibiting 11 β -HSD1 should therefore be selective for this isoform since potent inhibition of 11 β -HSD2 may result in sodium retention, hypokalemia, and hypertension.⁷

In the last decade, several classes of 11 β -HSD1 inhibitors have been identified by the pharmaceutical industry and academic groups.⁸ These included sulfonamides such as BVT.2733 or

* Corresponding authors.

E-mail addresses: Olivier.Venier@sanofi-aventis.com (O. Venier), Eric.Nicolai@sanofi-aventis.com (E. Nicolai).

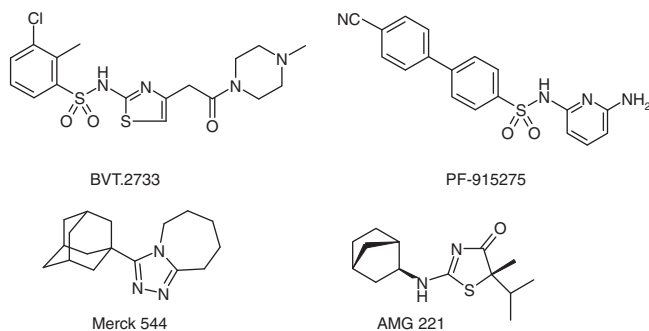


Figure 2. Representative 11β-HSD1 inhibitors.

PF-915275,^{9,10} triazoles such as the Merck compound 544,¹¹ and thiazolones such as Amgen compound AMG221 (Fig. 2).¹²

At the time we started our research program, few drug candidates had entered clinical trials: PF-915275 had been discontinued for formulation issues¹³ and BVT3498 was stopped for unknown reasons.¹⁴ Nevertheless, in 2008, proof of concept of therapeutic efficacy of 11β-HSD1 inhibition in type 2 diabetic patients has been obtained with INCB013739 showing improvement of blood glucose parameters and lipid profile.¹⁵ Furthermore, several classes of 11β-HSD1 inhibitors including INCB013739 displayed limited activity on rodent enzymes, making it difficult to assess them in appropriate animal models for optimal drug candidate selection. In metabolic disease pathogenesis, 11β-HSD1 activity is up-regulated in adipose tissue and the liver, thus inhibition in both tissues is a likely prerequisite for producing significant benefits.¹⁶ In order to identify new drug candidates with an optimal PK/PD profile we focused our efforts on compounds displaying inhibition of both human and rodent enzymes, thus allowing early ex vivo testing in rodent.

A HTS campaign using the Sanofi-aventis chemical library and sorting of the resulting hits resulted in the identification of two potent and selective inhibitors, compounds **1** and **2a**, which displayed mixed human/rodent 11β-HSD1 activity and good selectivity over 11β-HSD2 (Fig. 3).

Unfortunately, these compounds include an imidazole moiety which is known as a potential CYP3A4 binder¹⁷ and experimental data confirmed that both **1** and **2a** were strong CYP3A4 inhibitors ($IC_{50} < 1 \mu M$). To overcome this issue,¹⁸ we prepared a series of analogs where the imidazole ring was replaced by alternative surrogate heterocyclic moieties (Table 1). The synthesis of compounds **2a–m** is depicted in Schemes 1–3.

Compound activity was measured in vitro using recombinant human (h) and mouse (m) 11β-HSD1 enzymes. The conversion of radiolabeled cortisone into cortisol was detected using an anti-cortisol antibody in a miniaturized scintillation proximity assay (SPA).³¹ As shown in Table 1, changing the position of one nitrogen in the imidazole ring of **2a** resulted in a dramatic loss of activity (**2b**), indicating a key interaction between this nitrogen and the protein. No improvement was observed with the imidazoline **2c**.

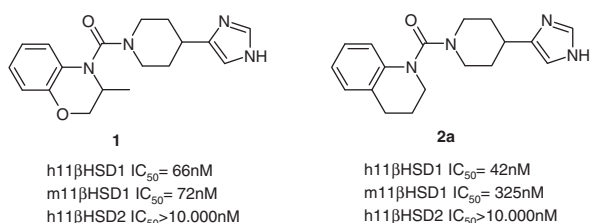


Figure 3. Structure and inhibitory activities of lead compounds **1** and **2a**.

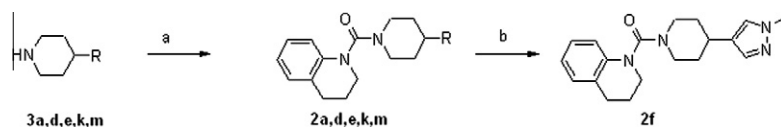
Table 1
Variations of the tetrahydroquinoline urea: compounds **2a–m**

Compound	R	h/m 11β-HSD1 IC_{50} (nM)
2a		42/325
2b		>2000/ND
2c		>2000/ND
2d		127/1000
2e		20/113
2f		436/ND
2g		>2000/ND
2h		>2000/ND
2i		378/ND
2j		93/ND
2k		>2000/ND
2l		>2000/ND
2m		66/73

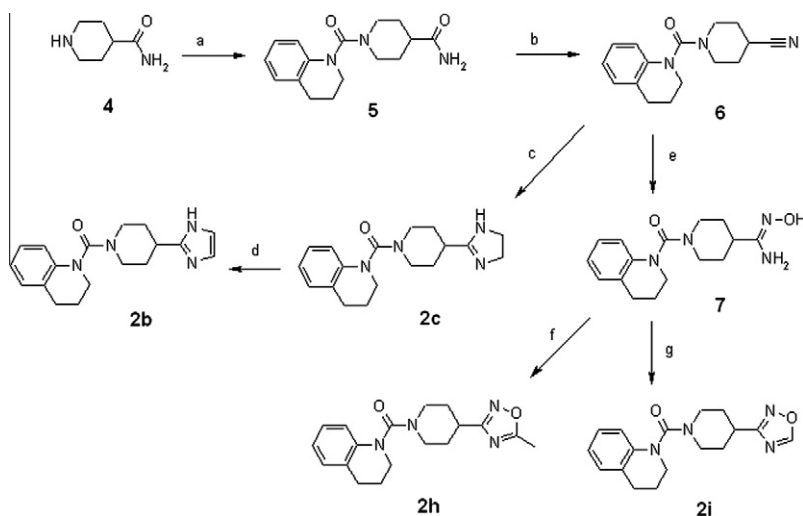
ND: not determined.

The oxadiazole derivatives **2g–k** showed variable inhibition potency depending of the structure and substitution of the oxadiazole with the 1,2,4-oxadiazole derivative **2j** being the most potent. The 3-pyridyl derivative **2m** was in the same range of activity as **2a** with an IC_{50} of 66 nM. Replacement by an oxazole (**2k**) and a triazole (**2l**) dramatically decreased the activity. Finally, the 4-substituted pyrazole derivative **2e** displayed a twofold potency enhancement compared to **2a**. Introduction of a methyl group at the nitrogen atom of the pyrazole (**2f**) led to a 20-fold loss in potency. This result highlighted in part the favorable effect of a hydrogen bond donor at that position (H-bond interaction between the NADPH cofactor and the heterocyclic NH was confirmed by the X-ray co-crystal structure, see Fig. 4a). In addition, this effect can be in part associated with unfavorable steric interaction. As expected, non-imidazole compounds **2e–f** displayed reduced CYP3A4 inhibitory activity with IC_{50} 's above 10 μM . This first round of optimization allowed the identification of **2e** as a new lead with potent activity in human and rodent enzymes and no CYP3A4 inhibition issue and prompted us to consider the pyrazole moiety as the best imidazole surrogate even though **2e** displayed limited metabolic stability (%lab: 57/79 in human/mouse liver microsomes).³²

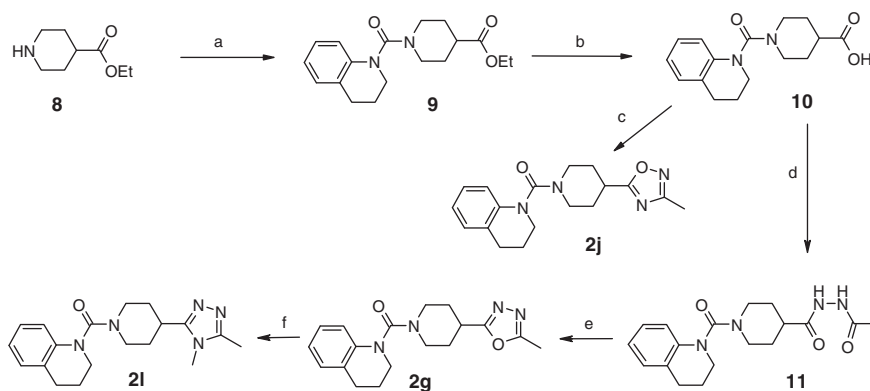
In order to check if piperidine was the optimal heterocyclic spacer, we kept the pyrazole moieties of **2d–e** and assessed different piperidine replacements. We first evaluated the tropane



Scheme 1. Synthesis of inhibitors **2a,d,e,k** and **2f**. R is as defined in Table 1. Reagents and conditions: (a) 0 °C, triphosgene,¹⁹ Et₃N, 1,2,3,4-tetrahydroquinoline, CH₂Cl₂ then compound **3** (**2d** 87%, **2k** 41%), or *p*-nitrophenyl(1,2,3,4-tetrahydroquinoline)carbamate,²⁰ Et₃N, CH₂Cl₂ (**2e**, 28%) or methylimidazolium (1,2,3,4-tetrahydroquinoline)carbamate iodide,²¹ Et₃N, CH₂Cl₂ (**2a** 16%); (b) **2e**, BEMP supp., MeI, CH₃CN, 55%.²²



Scheme 2. Synthesis of inhibitors **2b,c,h,i**. Reagents and conditions: (a) triphosgene, Et₃N, 2-tetrahydroquinoline, CH₂Cl₂/CH₃CN then compound **4**, 100%; (b) TFAA,²³ Et₃N, CH₂Cl₂, 0 °C, 82%; (c) ethylenediamine, S8, reflux, 46%;²⁴ (d) MnO₂, dioxane, 41%;²⁵ (e) ethanalamine HCl, Et₃N, MeOH, reflux, 84%; (f) acetyl chloride, DMF, 43%;²⁶ (g) triethyl orthoformate, reflux, 43%.²⁷



Scheme 3. Synthesis of inhibitors **2g,j,l**. Reagents and conditions: (a) diposgene, Et₃N, 2-tetrahydroquinoline, CH₂Cl₂ then compound **8**, 100%; (b) NaOH, EtOH, 50 °C, 93%; (c) *N*-hydroxy-acetamide, TBTU, HOBT, DIPEA, DMF, 95 °C, 46%;²⁸ (d) acetic acid hydrazide, EDC, HOBT, Et₃N, CH₂Cl₂/CH₃CN, 33%; (e) supp. BEMP, TsCl, THF, reflux, 51%;²⁹ (f) methylamine HCl, methylamine 2 M in MeOH, 130 °C, microwave, 31%.³⁰

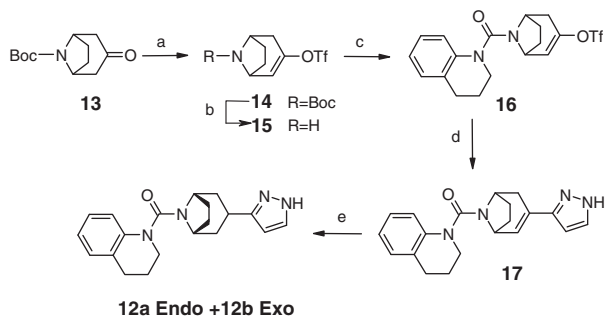
analogs **12a** and **12b**, the synthesis of which is illustrated in Scheme 4. This chemical scheme is an alternative strategy, where the pyrazole group is introduced after urea formation. The preparation of the pyrrolidine analog **12c** is illustrated in Scheme 5. In this synthetic scheme, the carbon–carbon bond formation between the pyrrolidine and the pyrazole is performed before the urea formation step.

The effect of these piperidine modulations on human/mouse enzyme inhibition and metabolic stability are summarized in Table 2. The endo tropane derivative **12a** compared favorably with its piperidine analog **2d**. On the other hand, the *exo* conformer **12b** is fivefold less potent on human enzyme. The pyrrolidine derivative **12c** displayed the most potent activity in both human (IC₅₀ = 4 nM) and mouse enzyme (IC₅₀ = 25 nM). However, it exhibited insufficient metabolic stability for *in vivo* testing.

As the benzylic position of the tetrahydroquinoline was identified as a spot for oxidative metabolism we tried to modulate this position by introduction of steric hindrance or heteroatoms in order to increase the metabolic stability.

Compounds **23a** and **23c** were obtained from commercially available building blocks using the synthetic route presented in Scheme 1. The synthesis of the spirocyclopropyl derivative **23b** is depicted in Scheme 6. The synthetic route for preparing tetrahydroquinoxaline derivatives **23d–e** is shown in Scheme 7.

The effect of tetrahydroquinoline modifications on human/mouse inhibition potency and metabolic stability are presented in Table 3. The dimethyl derivative **23a** displayed a very potent enzymatic inhibition of human and mouse 11β-HSD1 but still a very low metabolic stability, showing that hindering the metabolically labile benzylic position had no effect and that metabolic



Scheme 4. Synthesis of inhibitors **12a** and **b**. Reagents and conditions: (a) LDA, THF, *N*-phenylbis(trifluoromethanesulfonamide), -78°C , 77%; (b) HCl 4 M dioxane, 100%;³³ (c) triphosgene, Et₃N, 1,2,3,4-tetrahydroquinoline, CH₂Cl₂ then compound **15**, 88%; (d) Pd(PPh₃)₄, 1*H*-pyrazole-3-boronic acid, NaHCO₃, DME, 90 °C, 58%; (e) H₂, Pd/C, EtOH, 18%.

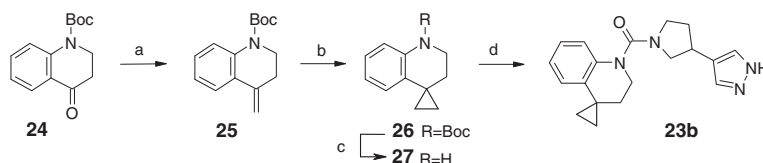
ability was more likely due to high lipophilicity. This was confirmed by the cyclopropyl derivative **23b** which displayed the same features as **23a**.

Table 2

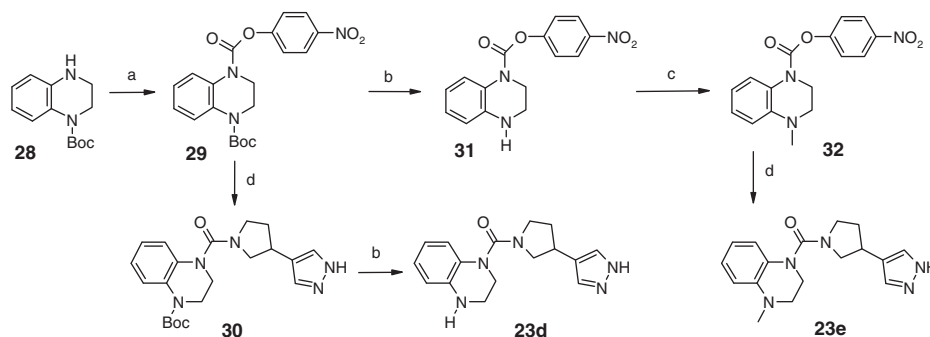
Modulation of the piperidine moiety: compounds **12a–c**

Compound	Pyrazole	Het	11β-HSD1 IC ₅₀ (nM) h/m	% Metabolic lability h/m
12a			40/51	ND/ND
12b			200/ND	ND/ND
12c			4/25	48/74

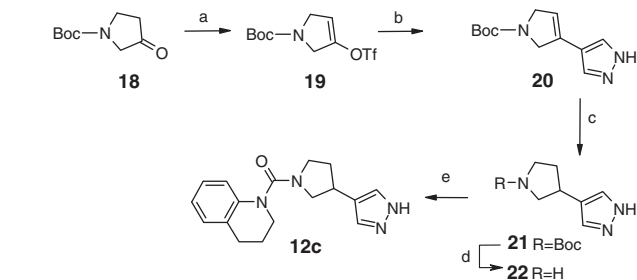
ND: not determined.



Scheme 6. Synthesis of inhibitor **23b**. Reagents and conditions: (a) PPh₃MeBr, *t*-BuOK, THF, reflux, 79%; (b) Et₂Zn, ClCH₂I, Et₂O;³⁴ (c) HCl 4 M dioxane, 21% two steps; (d) triphosgene, Et₃N, CH₂Cl₂ then compound **22**, 21%.



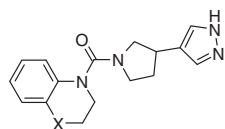
Scheme 7. Synthesis of inhibitors **23d–e**. Reagents and conditions: (a) 4-nitrophenyl chloroformate, TEA, THF, 100%; (b) 4 M HCl in dioxane, 100%; (c) NaBH(OAc)₃, formaldehyde, CH₂Cl₂, 46%; (d) compound **22**, THF, 100 °C, microwave, 45–80%.



Scheme 5. Synthesis of inhibitor **12c**. Reagents and conditions: (a) LiHMDS, *N*-phenylbis(trifluoromethanesulfonamide), THF, -78°C , 28%; (b); Pd(PPh₃)₄, *N*-Boc-pyrazole-4 boronic acid pinacol ester, K₂CO₃, DME, 90 °C, 85%; (c) H₂, Pd/C, EtOH, 81%; (d) HCl 4 M dioxane, 100%; (e) triphosgene, Et₃N, 1,2,3,4-tetrahydroquinoline, CH₂Cl₂ then compound **22**, 58%.

On the other hand, replacing the benzylic methylene by an oxygen atom in **23c** improved metabolic stability while keeping good inhibitory activity of the human enzyme but not of that of the rodent. Replacement of the oxygen by a nitrogen as in **23d** further enhanced the metabolic stability over **12c** (13% vs 48% lability in

Table 3
Modulation of the tetrahydroquinoline ring: compounds **23a–e**



Compound	X	11 β -HSD1 IC ₅₀ (nM) h/m	% Metabolic lability h/m	CaCO ₂ Permeability (10 ⁻⁷ cm s ⁻¹)
12c	-CH ₂ -	4/25	48/74	277
23a		8/7	94/ND	362
23b		18/21	78/79	ND
23c	-O-	27/490	4/44	281
23d	-NH-	7/55	13/30	139
23e	-NMe-	9/26	70/ND	ND

ND: not determined.

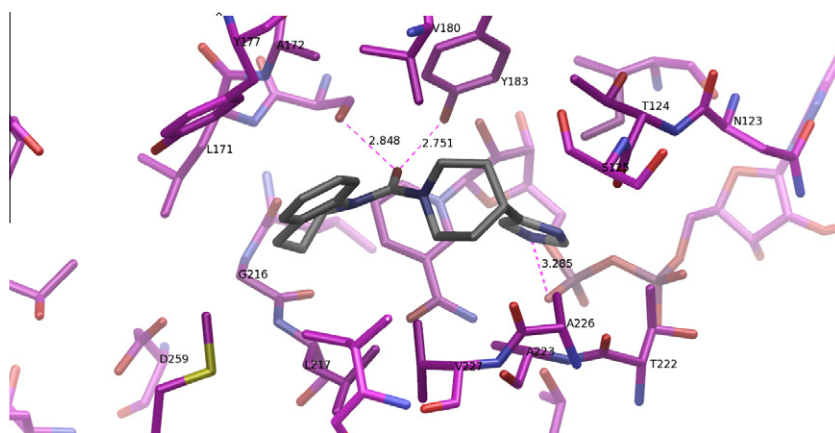


Figure 4a. Crystal structure of human 11 β -HSD1 with compound **2a**. The key hydrogen bonding interactions of **2a** to the enzyme are shown as magenta dashed lines with distances given in angstroms. The color scheme is red for oxygen atoms, blue for nitrogen atoms, maroon for phosphorus atoms and yellow for sulfur atoms. Carbon atoms are dark gray for the ligand and purple for protein and NADP cofactor. Water molecules are omitted for clarity. Resolution is 2.72 Å.

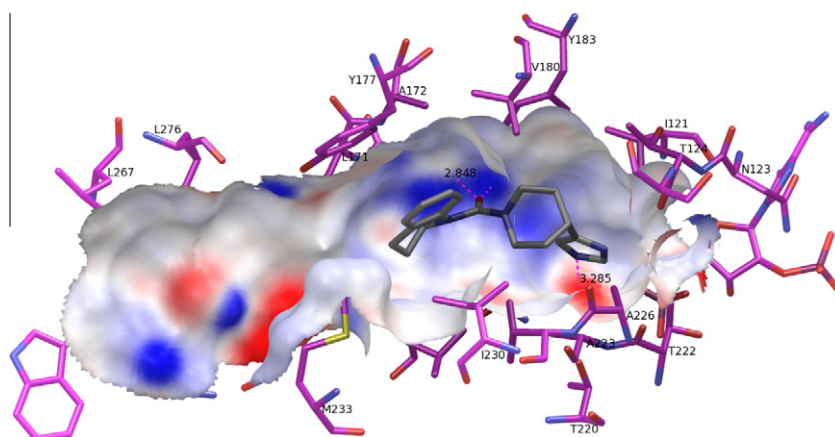
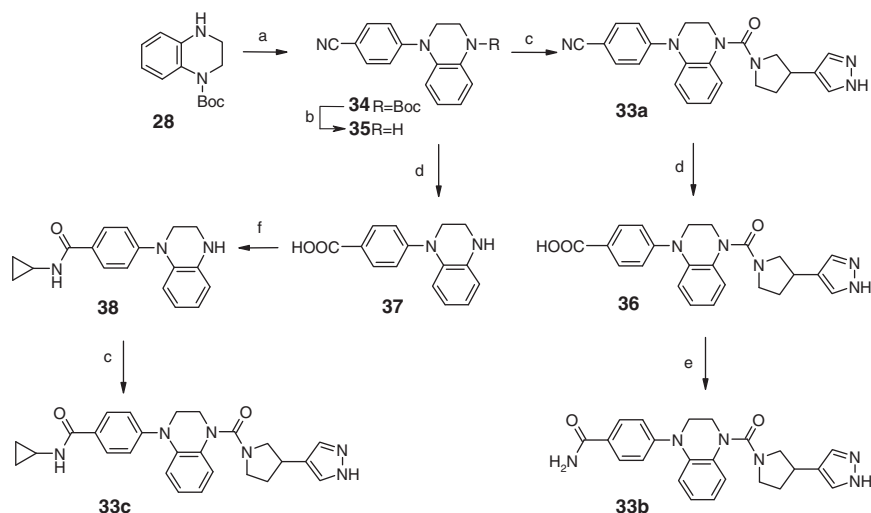


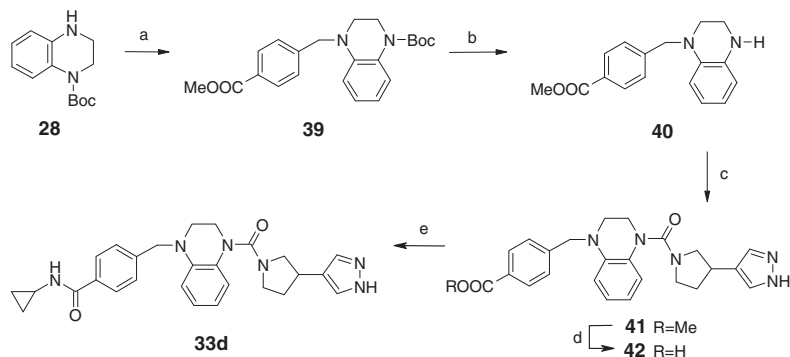
Figure 4b. X-ray crystal structure of compound **2a** in human 11 β -HSD1. The shape of the binding site is shown as a Connolly surface with the electrostatic potential as calculated by the MAESTRO software³⁶ being mapped onto the surface. Areas of positive potential are shown in blue, areas of negative potential are shown in red.

human liver microsomes, 30% vs 74% lability in mouse liver microsomes at 20 min), maintained an excellent potency on both human and mouse enzymes and gave a good estimated intestinal permeability. The *N*-methyl derivative **23e** showed a drop in metabolic stability while keeping a good inhibitory activity.

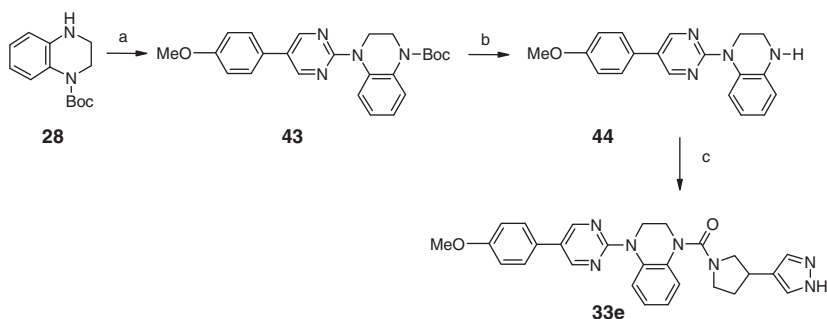
Compound **23d** was considered a good lead to be assessed in a pharmacodynamic assay in mice in order to determine its ability to inhibit 11 β -HSD1 in target tissues.³⁵ Despite a favorable in vitro ADME profile, **23d** did not show any inhibition of 11 β -HSD1 in the liver and adipose tissue at 2 h post administration to mice at



Scheme 8. Synthesis of inhibitors **33a,b,c**. Reagents and conditions: (a) 4-fluorobenzonitrile, *t*-BuOK, DMSO, 59%; (b) 4 M HCl in dioxane, 100%; (c) triphosgene, Et₃N, CH₂Cl₂ then compound **22**, 22–48%; (d) 10 N aq HCl, 100 °C, 15–97%; (e) aq NH₃, EDC, HOBT, dioxane, 22%; (f) cyclopropylamine, Et₃N, EDC, HOBT, dioxane, 78%.



Scheme 9. Synthesis of inhibitor **33d**. Reagents and conditions: (a) NaBH(OAc)₃, methyl 4-formylbenzoate, CH₂Cl₂, 63%; (b) 4 M HCl in dioxane, 93%; (c) triphosgene, Et₃N, CH₂Cl₂ then compound **22**, 66%; (d) LiOH, H₂O, THF, MeOH, 74%; (e) cyclopropylamine, DIPEA, EDC, HOBT, CH₂Cl₂, 22%.



Scheme 10. Synthesis of inhibitor **33e**. Reagents and conditions: (a) LiHMDS, THF, 2-chloro-5-(4-methoxy-phenyl)-pyrimidine, 56%; (b) 4 M HCl in dioxane, 49%; (c) triphosgene, Et₃N, CH₂Cl₂ then compound **22**, 75%.

30 mg/kg per os. As reasons for this lack of activity could be high clearance and/or inappropriate tissue distribution, modulation of the physico-chemical properties of the tetrahydroquinoxaline series was carried out in order to identify compounds with increased exposure in fat and the liver. For this, we considered possibilities for extending the scaffold.

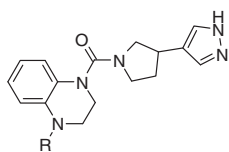
In order to identify appropriate intervention points from which we could extend **23d**, we used a co-crystal structure of compound **2a** bound to human 11 β -HSD1 (pdb code 3QQP). This structure indicates that the inhibitor **2a** binds to the steroid binding site with its central urea interacting with the key residues Tyr183 and

Ser170 responsible for substrate ketone reduction (Fig. 4a). The tetrahydroquinoxaline moiety of **2a** is oriented toward a solvent access channel which makes an extension possible from its benzylic position (Fig. 4b). This prompted us to use the nitrogen atom of **23e** as an attachment point to extend molecules into the solvent access channel.

The synthesis of extended compounds **33a–g** is depicted in Schemes 8–10.

The effects of tetrahydroquinoxaline extension are summarized in Table 4. Gratifyingly, our hypothesis was confirmed experimentally with the first extended compound, **33a**, which retained good

Table 4
Extension of the tetrahydroquinoxaline urea: compounds **33a–e**



Compound	X	11 β -HSD1 IC ₅₀ (nM) h/m	% Metabolic lability h/m	CaCO ₂ Permeability (10 ⁻⁷ cm s ⁻¹)
33a		37/75	59/54	190
33b		100/55	ND/ND	ND
33c		67/90	25/36	14
33d		73/108	79/60	ND
33e		43/49	40/10	194

ND: not determined.

Table 5
Ex vivo inhibition of 11 β -HSD1 activity in target tissues after oral administration of compound **33e** at 30 mg/kg to mice

	Liver	Fat
% Inhibition 2 h post dosing	90%	70%

mixed human/mouse inhibitory activity.³⁷ Unfortunately, the metabolic lability of **33a** was too high for ex vivo evaluation. Increasing the polarity of the molecule by changing the cyano group of **33a** into a primary amide led to **33b** which displayed reduced potency against the human enzyme. Substitution of the amide with a cyclopropyl provided **33c** which restored activity on the human enzyme and improved metabolic stability. Unfortunately introduction of such a polar amide moiety led to a drop in intestinal permeability (amide **33b,c** vs cyano **33a**). The benzylic analog **33d** was equipotent to **33c** but displayed poor metabolic stability. Further extension by introduction of a bi-aryl moiety gave rise to **33e** which turned out to be a potent inhibitor (IC₅₀ <50 nM on human and mouse enzymes) with a high permeability value, and low metabolic lability in mouse and human microsomes. Furthermore, additional experiments showed that **33e** was selective over 11 β -HSD2 (IC₅₀ >10 μ M).

Thus the extended lead **33e** displayed appropriate in vitro activity on both human and rodent enzymes, and favorable ADME and selectivity profiles for further characterization in animals.

It was therefore used as a tool to validate the 'extended compound' hypothesis. We determined its ex vivo activity in mouse target tissues (Table 5). Interestingly, **33e** produced a significant inhibition of 11 β -HSD1 in both the liver and fat tissue, 2 h after oral administration at 30 mg/kg. Compound **33e** thus constituted a satisfactory starting point to elaborate further optimization aimed at increasing the duration of action in both target tissues to give an optimal drug candidate.

In conclusion, starting from compact imidazolylpiperidine ureas with strong CYP3A4 inhibition liability, we moved to pyrazolylpyridine urea analogs devoid of CYP3A4 issues but with poor ex vivo activity in mouse.

We then took advantage of structural biology data to design and assay new extended compounds which addressed the solvent access channel of the protein. These extended compounds not only retained potent inhibitory activity on both human and rodent enzymes but displayed improved metabolic stability and ex vivo activity in target tissues as illustrated by the lead compound **33e**. Further optimization of **33e** has been performed (results to be published) leading to identification of new drug candidates with an optimal PK/PD profile.³⁸

References and notes

- Tomlinson, J. W.; Walker, E. A.; Bujalska, I. J.; Draper, N.; Lavery, G. G.; Cooper, M. S.; Hewison, M.; Stewart, P. M. *Endocr. Rev.* **2004**, *25*, 831.
- (a) Thieringer, R.; Hermanowski-Vosatka, A. *Expert Rev. Cardiovasc. Ther.* **2005**, *3*, 911; (b) Wamil, M.; Seckl, J. R. *Drug Discovery Today* **2007**, *12*, 504.
- (a) Kotelevtsev, Y.; Holmes, M.; Burchell, A.; Houston, P. M.; Schmoll, D.; Jamieson, P.; Best, R.; Brown, R.; Edwards, C. R. W.; Seckl, J. R.; Mullins, J. J. *Proc. Natl. Acad. Sci. U.S.A.* **1997**, *94*, 14924; (b) Masuzaki, H.; Paterson, J.; Shinyama, H.; Morton, N. M.; Mullins, J. J.; Seckl, J. R.; Flier, J. S. *Science* **2001**, *294*, 2166.
- (a) Barf, T.; Vallgård, J.; Emond, R.; Häggström, C.; Kurz, G.; Nygren, A.; Larwood, V.; Mosialou, E.; Axelsson, K.; Olsson, R.; Engblom, L.; Edling, N.; Rönquist-Nii, R.; Öhman, B.; Alberts, P.; Abrahamse, L. *J. Med. Chem.* **2002**, *45*, 3813; (b) Alberts, P.; Engblom, L.; Edling, N.; Forsgren, M.; Klingstrom, G.; Larsson, C.; Rönquist-Nii, Y.; Ohman, B.; Abrahamson, L. *Diabetologia* **2002**, *45*, 1528; (c) Yeh, V. S. C.; Kurukulasuriya, R.; Fung, S.; Monzon, K.; Chiou, W.; Wang, J.; Stolarik, D.; Imade, H.; Shapiro, R.; Knourek-Segel, V.; Bush, E.; Wilcox, D.; Nguyen, P. T.; Brune, M.; Jacobson, P.; Link, J. T. *Bioorg. Med. Chem. Lett.* **2006**, *16*, 5555; (d) Wan, Z. K.; Chenail, E.; Xiang, J.; Li, H. Q.; Ipek, M.; Bard, J.; Svenson, K.; Mansour, T. S.; Xu, X.; Tian, X.; Suri, V.; Hahm, S.; Xing, Y.; Johnson, C. E.; Li, X.; Qadri, A.; Panza, D.; Perreault, M. J.; Tobin, F.; Saiah, E. *J. Med. Chem.* **2009**, *52*, 5449.
- (a) Paulmyer-Lacroix, O.; Boullu, S.; Oliver, C.; Alessi, M. C.; Grino, M. *J. Clin. Endocrinol. Metab.* **2002**, *87*, 2701; (b) Kannisto, K.; Pietiläinen, K. H.; Ehrenborg, E.; Rissanen, A.; Kaprio, J.; Hamsten, A.; Yki-Järvinen, H. *J. Clin. Endocrinol. Metab.* **2004**, *89*, 4414; (c) Rask, E.; Olsson, T.; Söderberg, S.; Andrew, R.; Livingstone, D. E.; Johnson, O.; Walker, B. R. *J. Clin. Endocrinol. Metab.* **2001**, *86*, 1418.
- Van Uum, S. H.; Lenders, J. W.; Hermus, A. R. *Semin. Vasc. Med.* **2004**, *4*, 121.
- Kotelevtsev, Y. V.; Brown, R. W.; Fleming, S.; Kenyon, C.; Edwards, C. R. W.; Seckl, J. R.; Mullins, J. J. *J. Clin. Invest.* **1999**, *103*, 683.
- Hale, C.; Wang, M. *Mini-Rev. Med. Chem.* **2008**, *8*, 702.
- Barf, T.; Vallgård, J.; Emond, R.; Häggström, C.; Kurz, G.; Nygren, A.; Larwood, V.; Mosialou, E.; Axelsson, K.; Olsson, R.; Engblom, L.; Edling, N.; Rönquist-Nii, Y.; Öhman, B.; Alberts, P.; Abrahamson, L. *J. Med. Chem.* **2002**, *45*, 3813.
- Bhat, B. G.; Hosea, N.; Fanjul, A.; Herrera, J.; Chapman, J.; Thalacker, F.; Stewart, P. M.; Rejto, P. *J. Pharmacol. Exp. Ther.* **2007**, *324*, 299.

11. Gu, X.; Dragovic, J.; Koo, G. C.; Koprak, S. L.; LeGrand, C.; Mundt, S. S.; Shah, K.; Springer, M. S.; Tan, E. Y.; Thieringer, R.; Hermanowski-Vosatka, A.; Zokian, H. J.; Balkovec, J. M.; Waddell, S. T. *Bioorg. Med. Chem. Lett.* **2005**, *15*, 5266.
12. Caille, S.; Cui, S.; Hwang, T. L.; Wang, X.; Faul, M. M. *J. Org. Chem.* **2009**, *74*, 3833.
13. www.clinicaltrials.gov; August 4th, 2010.
14. Wess, L. Biovitrum replenishes. *BioCentury* 2005, March 28, A13.
15. Gathercole, L. L.; Stewart, P. M. *J. Steroid Biochem. Mol. Biol.* **2010**, *122*, 21.
16. Webster, S. P.; Ward, P.; Binnie, M.; Craigie, E.; McConnell, K. M. M.; Sooy, K.; Vinter, A.; Seckl, J. R.; Walker, B. R. *Bioorg. Med. Chem. Lett.* **2007**, *17*, 2838.
17. Tang, C.; Chiba, M.; Nishime, J.; Hochman, J. H.; Chen, I.-W.; Williams, T. M.; Lin, J. H. *Drug Metab. Dispos.* **2000**, *28*, 680.
18. Hooper, W. D. In *Handbook of Drug Metabolism*; Woolf, T. F., Ed.; Marcel Dekker: New York, 1999; pp 229–238.
19. Waal, N. D.; Yang, W.; Oslob, J. D.; Arkin, M. R.; Hyde, J.; Lu, W.; McDowell, R. S.; Yu, C. H.; Raimundo, B. C. *Bioorg. Med. Chem. Lett.* **2005**, *15*, 983.
20. Mehrotra, M. M.; Heath, J. A.; Rose, J. W.; Smyth, M. S.; Seroogy, J.; Volkots, D. L.; Ruhter, G.; Schotten, T.; Alaimo, L.; Park, G.; Pandey, A.; Scarborough, R. M. *Bioorg. Med. Chem. Lett.* **2003**, *12*, 1103.
21. Batey, R. A.; Santhakumar, V.; Yoshina-Ishii, C. S.; Taylor, D. *Tetrahedron Lett.* **1998**, *39*, 6267.
22. Xu, W.; Mohan, R.; Morrissey, M. M. *Bioorg. Med. Chem. Lett.* **1998**, *8*, 1089.
23. Iyobe, A.; Uchida, M.; Kamata, K.; Hotei, Y.; Kusama, H.; Harada, H. *Chem. Pharm. Bull.* **2001**, *49*, 822.
24. Mirkhani, V.; Moghadam, M.; Tangestaninejada, S.; Kargara, H. *Tetrahedron Lett.* **2006**, *47*, 2129.
25. DeWald, H. A.; Beeson, N. W.; Hershenson, F. M.; Wise, L. D.; Downs, D. A.; Heffner, T. G.; Coughenour, L. L.; Pugsley, T. A. *J. Med. Chem.* **1988**, *31*, 454.
26. Cheng-Ming, C.; Ming-Shiu, H.; Min-Tsang, H.; Chun-Wei, K.; Suja, T. D.; Jen-Shin, S.; Hua-Hao, C.; Yu-Sheng, C.; Kak-Shan, S. *Org. Biomol. Chem.* **2008**, *6*, 3399.
27. Palin, R.; Clark, J. K.; Evans, L.; Houghton, A. K.; Jones, P. S.; Prosser, A.; Wishart, G.; Yoshiizumi, K. *Bioorg. Med. Chem.* **2008**, *16*, 2829.
28. Poulain, R. F.; Tartar, A. L.; Déprez, B. P. *Tetrahedron Lett.* **2001**, *42*, 1495.
29. Brain, C. T.; Brunton, S. A. *Synlett* **2001**, 382.
30. Olson, S.; Aster, S. D.; Brown, K.; Carbin, L.; Graham, D. W.; Hermanowski-Vosatka, A.; LeGrand, C. B.; Mundt, S. S.; Robbins, M. A.; Schaeffer, J. M.; Slossberg, L. H.; Szymonifka, M. J.; Thieringer, R.; Wright, S. D.; Balkovec, J. M. *Bioorg. Med. Chem. Lett.* **2005**, *15*, 4359.
31. The standard error for compd **33e** tested in nine separate assays is representative of the error in this enzymatic assay: geometric average of $IC_{50} = 43.4$ nM with a SEM (standard error to the mean) of 6.1 nM.
32. Compound is incubated 20 min with human or mouse hepatic microsomal fraction. Liability% result corresponds to disappearance of tested compound at the end of the experiment.
33. Comins, D. L.; Dehghani, A. *Tetrahedron Lett.* **1991**, *32*, 5697.
34. Charette, A. B.; Beauchemin, A. In *Organic Reactions*; Overman, L. E., Ed.; Wiley: New York, 2001; Vol. 58, pp 1–65.
35. Male C57Bl6/J from Charles River Laboratory, fed ad libitum under standard regimen with free access to water, were used in the study ($n = 5$ per group, 25–30 g at the time of experiment). The compound was administered orally at the dose of 30 mg/kg, as a suspension of Tween 80 in methylcellulose 0.6% (0.5:99.5; vol/vol), and under a volume of 10 mL/kg. Treated animals were sacrificed by cervical dislocation, and 50 mg of liver and 200 mg of subcutaneous fat tissue were removed for subsequent determination of 11 β -HSD1 activity. Tissue samples were immediately weighed, placed in ice-cold phosphate buffered saline (PBS) containing protease inhibitors, and then cut in small pieces before being incubated with radiolabeled 3H-cortisone. The reaction was stopped by adding 500 μ L of HCl 1 N/methanol (1:1, vol/vol) solution, and the supernatants were frozen on dry ice. After defrosting and a clarification step (centrifugation and filtration), the samples were injected on an HPLC (WATERS 2695 with a SunFire R column C18 3.5 μ m 4.6 \times 75 mm), coupled to a flow scintillation analyzer (Perkin-Elmer radiomatic 625T) to quantify the relative amount of 3H-cortisone (11 β -HSD1 substrate) and 3H-cortisol (11 β -HSD1 product).
36. Maestro 9.1, Schrödinger, LLC., New York, USA.
37. Hillgren, K. M.; Kato, A.; Brochardt, R. T. *Med. Res. Rev.* **1995**, *15*, 83.
38. Some of the molecules described in this article are included in WO2008000950 patent application.